Statistical analysis of random lasing emission properties in nematic liquid crystals

Sameh Ferjani,[1,2,3] Luca Sorriso-Valvo,[2] Antonio De Luca,[1,2,3] Valentin Barna,[1,2,3]
Rossana De Marco,[1] and Giuseppe Strangi[1,2,3]
[1]*Dipartimento di Fisica, Università della Calabria, and CNISM-Unità di Cosenza, Ponte P. Bucci, Cubo 31C, 87036 Rende (CS), Italy*
[2]*Regional Laboratory, LICRYL-INFM/CNR, Ponte P. Bucci, Cubo 33B, 87036 Rende (CS), Italy*
[3]*Center of Excellence, CEMIF.CAL, 87036 Rende (CS), Italy*
(Received 5 September 2007; revised manuscript received 26 March 2008; published 24 July 2008)

A statistical analysis of random lasing events observed in dye-doped nematic-liquid-crystal films is reported. The occurrence of random laser action in such complex fluids is due to residual resonances in the multiple scattering of spontaneously emitted photons. The Shannon entropy and a local-Poisson test are used here in order to quantitatively characterize the chaotic behavior of laser spikes and gain further understanding of the mechanisms underlying the lasing effect in strongly scattering organized fluids arising by an unexpected interplay of localization and amplification.

DOI: 10.1103/PhysRevE.78.011707 PACS number(s): 61.30.−v, 42.55.Zz, 05.45.Tp

I. INTRODUCTION

Since first proposed by Letokhov in 1968, who predicted that the combination of multiple scattering and light amplification would lead to a form of laser, lasing in disordered media has been a subject of intense theoretical and experimental studies [1,2]. Multiple-scattering phenomena have been observed in various systems such as powdered laser crystals, micro- and nanoparticles in laser dye solutions, and liquid-crystal-dye-infiltrated porous glasses. In these cases, the emission was shown to become narrow banded above a given pump energy threshold [3]. The physical mechanism behind random lasing can be explained by making an analogy to the electronic model proposed by Anderson in 1958 in the famous article "Absence of diffusion in certain random lattices" [4]. He described the vanishing of electron propagation in the regime of very strong multiple scattering due to interference in lattices where disorder was introduced as impurities. This concept served as a model for metal-insulator transitions. In an active random media, when the scattering is weak, the emission is spontaneous. When light scattering is enhanced above a critical value, recurrent light scattering events arise and the Ioffe-Regel criterion for localization, $kl_t < 1$ ($k=2p/\lambda$ is the wave vector and l_t is the scattering mean free path), is met. Nevertheless, in nature it is very difficult to find strongly scattering systems satisfying this stringent condition. A precursor of Anderson localization is the weak localization ($kl_t > 1$) manifested in multiple-scattering systems through coherent backscattering effects. The dwell time of light photons in such media can be increased, so that light is amplified by walking a longer random path inside the system. In the strong multiple-scattering regime, the system makes a transition into a localized state where light propagation is inhibited owing to survival of interference effects. In random lasers, it is exactly this strong multiple scattering inside the gain medium that provides the means for stimulated emission feedback. In 1996, Sapienza *et al.* performed scattering experiments on fully and partially disordered systems, demonstrating that interference effects manage to survive the scattering regime and give rise to enhancement of the light intensity in the backscattered direction—namely, the cone of coherent backscattering [5]. When optical scattering is strong, light may return to a scatterer from which it was scattered before and thereby form a closed-loop path that serves as a "random cavity." When light is trapped inside the gain medium long enough, the amplification along such a loop path can exceed the optical loss and the system starts to lase. As the pump energy is further increased, the balance between gain and loss becomes positive and additional narrow peaks appear in the emission spectrum. Such laser action is called diffusive or random lasing. Because random lasing modes come from the eigenstates of disordered systems, random lasers open a special door to study the interplay between localization and amplification. Recently, Strangi and co-workers [6,7] reported the first observations of random laser action in a partially ordered dye-doped nematic-liquid-crystal (NLC) system presenting various geometries. Backscattering experiments performed on NLCs show that the typical mean free path is a few tens of microns, ensuring that the presented samples were in multiple-scattering regime. In this paper, we investigate the random lasing emission properties in dye-doped nematic liquid crystals for different temperatures, below the nematic-isotropic transition, exploiting the optical feedback provided by the weak localization in such systems. In particular, a statistical study of the emitted photons is reported and a model is intended to explain the temperature- (versus time-) dependent behavior of the specklelike emission.

II. EXPERIMENT

The gain medium consists of a nematic-liquid-crystal mixture (BL001 by Merck) doped with 0.3% wt of Pyrromethene 597 dye (Exciton). The liquid-crystal bulk phase sequence is Cr −10 °C nematic 63 °C iso. The mixture was confined in a wedge cell constituted by two glass-ITO plates separated by Mylar spacers, with a thickness of 2 μm at one side and 0.2 mm at the other one. The glasses were treated with polyimide in order to induce a homogeneous alignment of the NLC molecules. The system was then optically pumped with 532 nm light from a frequency-doubled Nd:YAG laser (NewWave, Tempest 20). The pump light con-

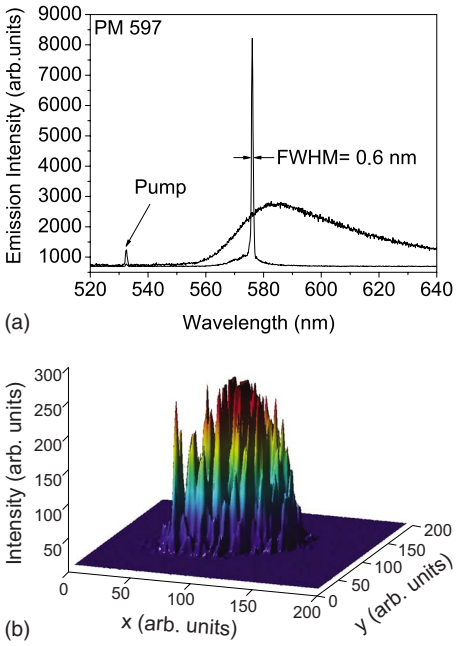

FIG. 1. (Color online) (a) Fluorescence and lasing spectra in a partially ordered dye-doped nematic liquid crystal confined in a wedge cell. Above a given threshold pump energy, discrete sharp peaks, having a full width at half maximum (FWHM) of only 0.6 nm, emerge from the residual spontaneous emission. (b) Far-field spatial distribution of the emission intensity shows a multitude of spatially overlapping lasing peaks.

sisted of a train of twenty 3-ns pulses focused into a 50-μm spot by means of a spherical lens. The emission properties were spectrally analyzed by means of a high-resolution optical multichannel charge-coupled-device (CCD) spectrometer (Jobin Yvon, Micro-HR). For low pump energy, the emission spectrum shows the typical spontaneous emission curve of the pyrromethene dye. When the pump intensity exceeds a certain threshold, several sharp lasing peaks emerge [Fig. 1(a)]. The far-field spatial distribution of the emitted light was captured with a high-sensitivity and -resolution CCD camera (PixelFlyQE by PCO), and it shows a series of spatially overlapping bright tiny spots which create a richly structured pattern typical of random lasers [Fig. 1(b)].

In order to gain further understanding of the multiple-scattering mechanism and its time- and temperature-dependent behavior, we statistically analyzed the emission intensity fluctuations. For this purpose, we collected the emitted light by means of a fast photodiode which was simultaneously triggered by the pump pulse. The signal was then sent to an oscilloscope and analyzed. Figure 2(a) depicts the temporal behavior of laser action in the case of highly ordered cholesteric and partially ordered nematic samples doped with fluorescent guest molecules. For a fixed pump power the cholesteric system shows very small variations in the lasing output intensity (the pump energy was kept fixed above the lasing threshold). Essentially, for each shot of the pump beam the system was in the "on" state. A totally different scenario is revealed in the case of the nematic dye-doped system: strong fluctuations of the emission intensity

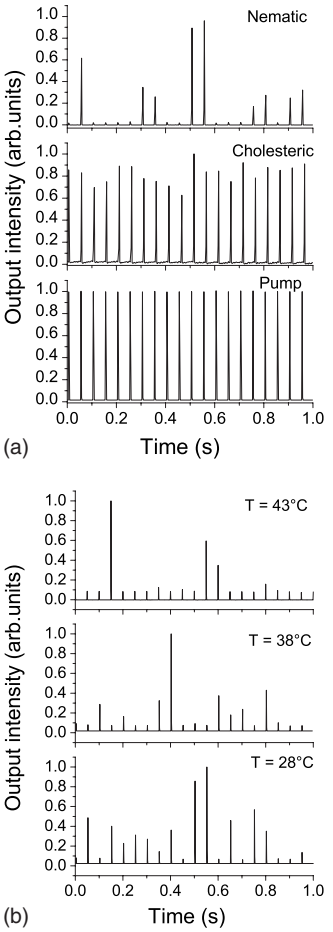

FIG. 2. (a) Pump and output emission intensities from both dye-doped cholesteric and dye-doped nematic samples as function of time. (b) The temporal emission intensity dependence on system temperature for a dye-doped NLC sample.

are measured for pump power above the lasing threshold. Irregular intermittent sequences of "on" and "off" states demonstrate a characteristic behavior for a random laser. Since the condition for lasing comes from a careful balance between gain and loss, it is clear that in this case the random walk inside the anisotropic medium does not gather enough gain at every pump pulse for the system to lase. Interestingly, upon increasing the temperature of the sample the system tends to present the off state more frequently. By increasing the temperature, the total scattering intensity slightly increases, but the coherent backscattering cone is lowered, emphasizing that the incoherent scattering component increases within the medium. The enhancement of incoherent scattering lowers the gain inside the system and decreases the probability of having lasing modes in this situation, since a larger number of spontaneously emitted photons are needed to act as seeds for the stimulated emission process.

III. CHARACTERIZATION: LOOKING FOR CORRELATIONS

To better understand the driving mechanisms within these systems, a statistical study has been performed. In particular,

we used two different statistical tools, already adopted in other contexts, to characterize the possible presence of memory in the system. As can be clearly seen by a look at Fig. 2(b) and as we have already mentioned, the diffusive laser action in dye-doped NLCs is rather irregular. It seems thus natural to investigate whether such irregularity is the result of a completely random process or if, instead, some form of correlation is present indicating the existence of an underlying mechanism in the system. The statistical description of the irregularity properties of the system could give useful information on several aspects, such as, for example, the temperature dependence mentioned above. Since, in this paper, we are interested in the irregularly alternating status of lasing (lasing or nonlasing in response to the pump), we chose to identify an "event" with the total intensity emitted by the system, as observed in correspondence with the pump pulse. Then, we set a threshold right above the noise level of the recorded signal and the pump level to separate the "nonlasing" events from the "lasing" ones. The result of such process is a signal made of "on" and "off" digits, indicating the status of emission of the system at each pump pulse. The presence of correlations, and thus of the memory effect, corresponds to evidence of some degree of regularities in the signal obtained through this procedure.

A. Shannon entropy

Let us now introduce the first statistical tool used in this work, known in the literature as Shannon (or information) entropy [8,10]. The regularity of a sequence of $N-1$ symbols (such as, for example, a word of binary digits), produced by any source, can be characterized through the ability in predicting the Nth symbol. In our case, the possible symbols are limited to the "on" and "off" states, so that the binary digits "0" and "1" are only needed to describe the sequence. We will give a brief description of the Shannon entropy in this case, recalling that the theory can be extended to an arbitrary number of different symbols. Given a sequence of N binary digits $s(i)$ $(i=1,\ldots,N)$, we introduce the probability $P(C_n)$ (namely, the occurrence rate within the sequence) of a particular "word" $C_n=(s(1),s(2),\ldots,s(n))$ of length n. Then, the entropy associated with a generic n-digit word can be defined as $H_n=-\Sigma_{\{C_n\}}P(C_n)\ln P(C_n)$, where the sum is computed over all possible combinations of length n. The quantity $h_n=H_{n+1}-H_n$, indicated as differential entropy, thus represents the average information provided by the $(n+1)$th digit, once the previous n digits are known. For a stationary source, the Shannon entropy can finally be defined as the limit for large values of n:

$$h_{sh}=\lim_{n\to\infty} h_n=\lim_{n\to\infty}\frac{H_n}{n}. \tag{1}$$

This quantity is a measure of the regularity of the sequence. For example, for a given regular (say, periodic) sequence, the information carried by the next digit after one period is zero, since full knowledge of the sequence is contained in the first period. The predictability of such a sequence is then trivially high, and the signal is completely correlated with long-range memory. On the contrary, if the sequence is chaotic, the information provided by knowledge of each digit can be high. For example, for a random realization—namely, if all digits have the same chance to be "0" or "1"—any next digit carries with it the same amount of information as the previous ones. Such a sequence is completely unpredictable, and neither memory nor correlations are present. In this case the limit (1) can be easily shown to be $h_{sh}=\ln 2$. Thus, the quantities defined so far represent a tool to describe the complexity of the source through the regularities of the emitted sequences. Note that although the theoretical Shannon entropy is defined as the limit to infinity of the word length, in real experiments the convergence of the limit (1) is normally already obtained for small values $n<10$.

TABLE I. For each temperature, the sequences size, the fraction of "on" states (in %), and the Shannon entropy are reported.

T (°C)	No. of events	No. of "1" events (%)	h_{sh}
26	2000	78	0.54
29	1999	71	0.60
32	1999	65	0.64
35	1854	39	0.67
38	1896	26	0.58
41	1971	14	0.42

Let us now consider our data set. In this work we focus on six data sets obtained by performing the same experiment at different values of the temperature in the interval between 26 °C and 41 °C. The experimental data have been reduced to 6 sequences of 2000 digits, each corresponding to the output state (lasing—that is, "on"—or nonlasing—that is, "off") as response to the excitation pulses. We underline that the choice of threshold is not relevant. In fact, different realizations of the analysis obtained with reasonable variations of the threshold gave the same results, so that we do not need to discuss it here. For each sequence made of "0" and "1" digits (see Table I), we then computed the quantities defined above—namely, the entropy H_n, the differential entropy h_n, and the Shannon entropy h_{sh}, using words of length up to $n=18$. The results are collected in Figs. 3 and 4. For comparison, in the same figures are reported, together with the 6 realizations at different temperatures, the results obtained using two artificial data sets. The first one is a regular sequence of alternating "0" and "1," while the second one is a completely random realization. Both sequences include 2000 digits, as for the observed strings. Looking at the top panel of Fig. 3, it is possible to observe that, for the regular string, there is no increase of information when the number n of digits of the words increases. This corresponds, as expected, to a vanishing differential entropy (bottom panel of Fig. 3) leading to $h_{sh}\sim 0$. The random case, conversely, displays a constant growth of entropy H_n with the number of digits, indicating that all of them bring the same amount of information (top panel of Fig. 3). This correspond to a constant differential entropy h_n (bottom panel of Fig. 3). In order to obtain a value of the Shannon entropy, we observe that a saturation of H_n, and consequently a vanishing trend for h_n, is reached for $n>5$, due to the finite size of our sequence. Thus, we can assume that the Shannon entropy is well rep-

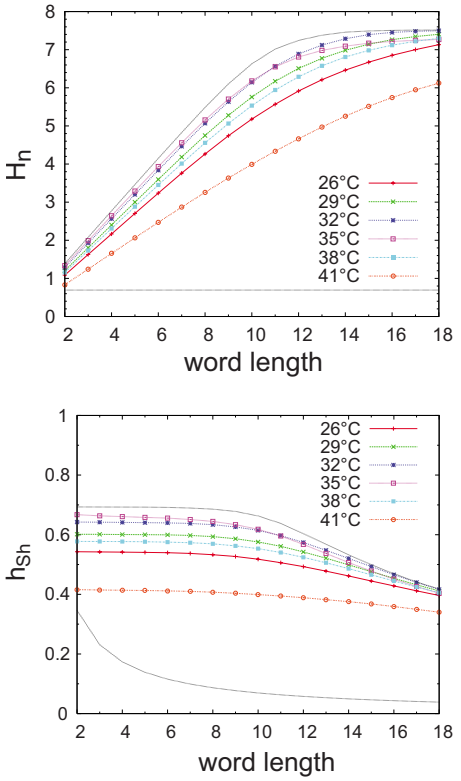

FIG. 3. (Color online) The values of the entropy H_n (top panel) and of the differential entropy h_n (bottom panel) as a function of the words length n. Different colors refer to the different data sets (the corresponding temperatures are indicated in the legend). For both panels, the black dotted lines represent the results obtained using the completely ordered artificial data set (the bottom curve) and the completely random realization (top curve).

resented by the constant region of the differential entropy h_n, with $n<5$. We decide, thereafter, to use the first value reported in the plot—namely, h_2—as a proxy for the Shannon entropy. The values of our estimates are displayed in Fig. 4. For the random case, the expected value $h_{sh}=\ln 2$ is obtained.

The experimental sequences, obtained from the different data sets, show a clear temperature dependence, accordingly

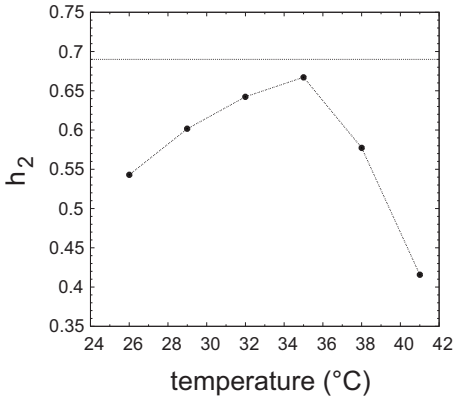

FIG. 4. The values of the differential entropy h_2 as a proxy for the Shannon entropy, measured at different temperatures. The dotted line shows the completely random value $H_2=0.69$.

with the probability variations reported in Table I. At low temperature, at which the string is mainly composed by "on" digits (see Table I), the entropy curve indicates that the system is chaotic, but with some degree of regularity. This is evidenced by the fact that the information entropy H_n grows more slowly than for the random case (Fig. 3). Moreover, the values of the Shannon entropy are somewhat smaller than the upper value $h_{sh}=\ln 2$ (see Fig. 4). Thus, the amount of information carried by each digit is small. As the temperature is increased, the number of "on" and "off" digits become comparable, so that for $T=35$ °C the Shannon entropy reaches its maximum value $h_{sh}=0.67$, very close to the completely chaotic value. For higher temperatures, the trend is reversed, and long "0" series are interrupted by sporadic "1" digits. Both the high-temperature and low-temperature configurations, which are almost undistinguishable as far as Shannon entropy is concerned, imply the presence of recurrent words of the same state (e.g., 000…0), which makes the system more predictable and the information carried by each digit smaller, so that the Shannon entropy decreases. The indication of high chaoticity is anyway still valid. It should be noted that the number of "on" states decreases very smoothly (indeed almost linearly) with temperature, varying from a mainly-on configuration to a mainly-off one. The dominating state changes from "on" to "off" at some point between 32 °C and 35 °C (see Fig. 4). By comparing the slopes before and after the inversion of the Shannon entropy trends, we notice that it decreases more rapidly with respect to the rise phase. It means that by increasing the temperature the number of excitation pulses, which actually create the conditions to have lasing, reduces more rapidly after the inversion point. In order to shine light on this point, a series of experiments have been planned in which we intend to use pure *LC* and compare with mixtures where some phase-separations could occur producing a rapid increase of the intensity of the incoherent scattering component.

B. Local Poisson test

As we have seen, the Shannon entropy analysis provides useful information that the system under study is highly chaotic, especially at intermediate temperatures. At high and low temperatures, there is the indication of presence of regularity of the gain mechanisms behind the laser spiking, mainly due to the occurrence of long periods of a stable state. One further piece of information is that the system chaoticity changes smoothly with temperature. However, it is desirable to gain more insight into the system and in particular into the specific features of chaos. This can be obtained, for example, by looking at correlations of the emitted pulses. Correlations are indeed related to some underlying mechanism, so that their presence in a signal indicates the nonstochasticity of the phenomenon. Let us now consider our experimental data as a succession of words made of the same digit. This corresponds to transform the strings in series of "0"-only or "1"-only words of variable length η, this last being defined as the number of consecutive identical digits. Thus, the persistence of the system in a given state (lasing or nonlasing) is concerned here. In order to investigate the presence of correla-

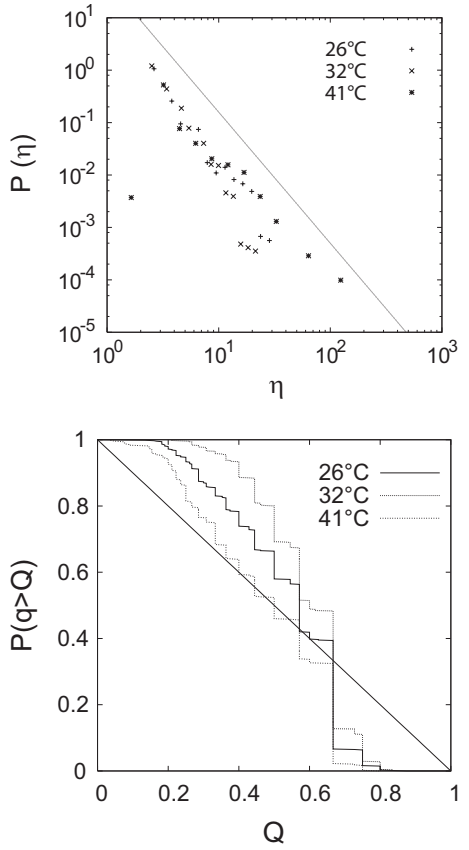

FIG. 5. Top panel: the PDF of the lengths η of words made of "1" only for three different values of the temperature. A power law is also plotted for reference. Bottom panel: the surviving function of the variable q (see text) for the same temperatures. The thin straight line $1-x$ represents the Poissonian, decorrelated case.

tions in the system, the probability distribution functions (PDFs) of the persistence lengths can be studied. Indeed, for a completely random process, such distributions are expected to be exponential. The presence of correlations, conversely, produces long-range power-law PDFs. This is an easy test to perform on our data. Figure 5 displays the distribution functions $P(\eta)$ obtained for three values of the temperature. PDFs are approximately power laws, indicating that the system is correlated not only at the border temperatures ($T=26$ °C and $T=41$ °C), but also at intermediate ones ($T=35$ °C).

Because of the limited size of the data sets, the PDFs shown in Fig. 5 might suffer from some uncertainties. We then performed a further analysis, which is less sensitive to the sample size. Such analysis was introduced some years ago in cosmology [9] and has been used more recently in astrophysical [10–12], geophysical [13], and econophysics [14] contexts.

Consider a sequence of m words, identified as the consecutive sets of identical symbol within the original binary sequence, as described above. The separation points between two successive words can be labeled with an index i and identified as an event. The events are thus defined as the change of state of the system from lasing to nonlasing and vice versa. For each event i, we use the length of the following or preceding next and second next words, which we call $L_1(i)$ and $L_2(i)$, respectively. The choice between the pair of words following event i and the pair preceding the same event is made in order to have the smallest $L_1(i)$. $L_1(i)$ and $L_2(i)$ are then the lengths of the two words following or preceding a given state change i. We then introduce a quantity, which we denote by q, which is nothing but the suitably normalized local word length

$$h(L_1(i),L_2(i)) = \frac{2L_1(i)}{2L_1(i)+L_2(i)}. \tag{2}$$

If the words lengths are randomly distributed, it can be shown that the probability density function $P(q)$ of the stochastic variable q defined above is uniformly distributed in $q \in [0,1]$. This correspond to having a linear decrease for the surviving function of $P(q)$—namely, $P(q \geq Q) = \int_Q^\infty P(q)dq = 1-Q$. To better understand the meaning of this tool, note that in a process where $L_2(i)$ are systematically smaller than $2L_1(i)$, clusters of state changes are present and the average value of q is greater than 1/2. On the contrary, when the process is characterized by increasing the persistence of the state, the average value of q is less than 1/2. Both cases indicate the presence of correlations in the signal. The test described above is thus a useful tool to discriminate between a sequence of random words and a sequence of correlated ones.

From the experimental strings, it is straightforward to calculate the surviving function $P(q \geq Q)$ and the test is easily performed. Figure 5 shows the surviving functions computed for the same three cases as $P(\eta)$. The stepwise shape of the surviving function is due to the discrete nature of the sequence and to the relatively small set of possible values of the lengths η. This results confirm that at all temperatures there is a relevant deviation from stochasticity, so that the presence of correlations is strong.

IV. CONCLUSIONS

The chaos of the amplification mechanism in dye-doped complex fluids has been quantitatively described through the Shannon entropy. The results have shown that it is highly chaotic and that a peculiar dependence on the temperature is present. In particular, we have shown that the chaoticity level increases when the temperature is increased, then reaches a peak at intermediate temperature, and finally decreases faster than in the growing regime. This could be due to the smooth changes in the relative number of lasing and nonlasing states in the signal. We then performed a test to verify the presence of correlations between the successive states of the random lasing. The results show clearly that correlations are observed in the emission properties of the dye-doped liquid crystal. On the other hand, unexpected coherence effects that are responsible for the optical feedback have already been observed in backscattering experiments using the system presented [5]. The correlations found in the lasing spikes could be related to the amplification mechanisms through the coherent scattering component that can present important fluctuations with long-range correlations. Our results suggest that for a better understanding of the basic physical mecha-

nisms of our systems, other tailored dye-doped complex fluids need to be explored. The comparison of statistical characteristics could reveal the entity of coherence effects in light localization processes.

APPENDIX

Coherent backscattering experiments were performed on dye-doped liquid crystals [BL001+DCM (4dicyanomethylene-2-methyl-6-p-dimethylaminostyryl-4H-pyran) dye molecules (exciton) 0.5 wt %] as a function of the temperature to gain understanding of the mechanisms behind the random lasing in our samples. Coherent backscattering (CBS) of light is a phenomenon in which partial waves traversing time-reversed (momentum-reversed) scattering paths interfere constructively in the backscattering direction, leading to the appearance of an intensity cone. An important result is the dependence of the coherent cone width on the transport mean-free-path length. The maximum angular cone width is the critical coherence angle obtained for the smallest total path length. The smallest average path length is l^*, yielding a cone width of $\theta_{\max} \approx \lambda / \sqrt{2l^*}$, which scales inversely with l^*.

The results reported in the Fig. 6 show a narrow (FWHM$\sim$6 mrad) backscattering cone at room temperature (RT) which slightly changes the width, but importantly changes the maximum intensity (enhancement factor) of the cone as the temperature increases. These experiments clearly prove the occurrence of weak localization through multiple scattering in our samples, since the measured average path length is about 10 μ. In addition, Fig. 6 shows that the enhancement factor of the coherent peak reduces as the temperature increases. This is due to thermally induced disorder (i.e., dielectric tensor fluctuations) giving rise to scattering regimes characterized by the lack of a time-reversed mate and thus reduces the observed enhancement factor. The different scattering regimes are pointed out by the slight enlargement of the coherent peak of the backscattering cone as the temperature increases by RT up to 60 °C.

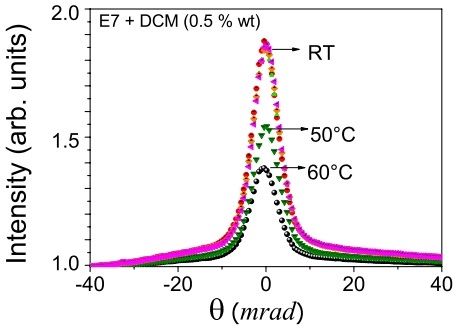

FIG. 6. (Color online) Coherent backscattering peaks as a function of temperature in a dye-doped liquid-crystal wedge cell. The enhancement factor reduces importantly as the temperature increases from RT up to 60 °C. The widths of the coherent peaks are slightly enlarged (from 6.1 to 6.8 mrad), indicating that the scattering regime changes.

[1] H. Cao, Y. G. Zhao, S. T. Ho, E. W. Seelig, Q. H. Wang, and R. P. H. Chang, Phys. Rev. Lett. **82**, 2278 (1999).
[2] D. Wiersma and S. Cavalieri, Nature (London) **414**, 708 (2001).
[3] H. Cao, J. Y. Xu, E. W. Seelig, and R. P. H. Chang, Appl. Phys. Lett. **76**, 2997 (2000).
[4] P. W. Anderson, Phys. Rev. **109**, 1492 (1958).
[5] R. Sapienza, S. Mujumdar, C. Cheung, A. G. Yodh, and D. Wiersma, Phys. Rev. Lett. **92**, 033903 (2004).
[6] G. Strangi, S. Ferjani, V. Barna, A. De Luca, C. Versace, N. Scaramuzza, and R. Bartolino, Opt. Express **14**, 7737 (2006).
[7] S. Ferjani, V. Barna, A. De Luca, C. Versace, and G. Strangi, Opt. Lett. **33**(6), 557 (2008).
[8] C. E. Shannon, Bell Syst. Tech. J. **27**, 379432 (1948).
[9] H. Bi, G. Corner, and Y. Chu, Astron. Astrophys. **218**, 19 (1989).
[10] G. Boffetta *et al.*, Phys. Rep. **356**, 367 (2002).
[11] G. Boffetta, V. Carbone, P. Giuliani, P. Veltri, and A. Vulpiani, Phys. Rev. Lett. **83**, 4662 (1999).
[12] F. Lepreti, V. Carbone, and P. Veltri, Astrophys. J. **555**, L133 (2001).
[13] V. Carbone, L. Sorriso-Valvo, A. Vecchio, F. Lepreti, P. Veltri, P. Harabaglia, and I. Guerra, Phys. Rev. Lett. **96**, 128501 (2006).
[14] A. Greco, V. Carbone, and L. Sorriso-Valvo, Physica A **376**, 480 (2007).